Available online at www.sciencedirect.com
SCIENCE DIRECT®
Chemical Physics 307 (2004) 147–155
Chemical Physics
www.elsevier.com/locate/chemphys

Molecular dynamics simulations of substrate channeling through an α–β barrel protein

Rommie Amaro, Zaida Luthey-Schulten *

Department of Chemistry, University of Illinois, 600 S. Mathews Avenue, A548 CLSL, Box 41-6, Urbana, IL 61801, USA

Received 9 March 2004; accepted 19 May 2004
Available online 19 June 2004

Abstract

Steered molecular dynamics simulations are used to probe the energetics of substrate channeling in an enzyme regulating histidine biosynthesis, imidazole glycerol phosphate synthase (IGPS). IGPS is a multidomain globular protein complex: the glutaminase domain hydrolyzes glutamine to form glutamate and ammonia, and is docked to the cyclase domain, a $(\beta/\alpha)_8$ barrel protein that completes the ring formation of imidazole glycerol phosphate. Recently, it has been suggested that this protein exploits its barrel structure to channel ammonia from one remote active-site to the other. The current work includes both domains, their substrates, ammonia, and explicit solvent. Compared to the apo-complex, the inclusion of substrates does indeed affect the barrier to ammonia entry into the channel as well its transport through the barrel. Based on bioinformatic data, we suggest an "open-gate" mechanism that has a low barrier to ammonia entry. We also perform the first systematic investigation of interface water molecules near the channel gate and argue that the optimum number of water molecules inside the channel is one.

1. Introduction

As the structural template for at least 21 different enzyme families [1], the α–β barrel fold is as versatile as it is ubiquitous. Over 900 Protein Data Bank structures share the eight parallel β strand, eight helix topological motif, making it one of the most populated folds to date. From a biological standpoint, it represents a paradigm for enzymatic design and, as such, has been the focus of numerous studies ranging from protein folding and design [2,3], to functional and structural evolution [4–6], to the mechanisms of enzyme catalysis [7,8] (for a recent review see [1,9]). Seemingly without exception, the reactions take place at the C-terminus end of the barrel. Recently, it has been suggested that the α–β barrel of imidazole glycerol phosphate synthase (IGPS), known as hisF, is used to transport small reaction intermediates from one active-site to another, thus presenting a novel function for this common fold [10–12]. The free energy landscape for ammonia conduction within the hisF barrel has been calculated but the previous analysis did not include bound substrates [10]. In the previous year, two α–β barrel proteins, triosephosphate isomerase [7] and IGPS from yeast [8,13], were crystallized with substrates. Invaluable insights can be gleaned from further investigating these substrate-bound protein systems; specifically, molecular dynamics simulations (MD) allow us to probe the system beyond the snapshot provided by the crystal structure. By applying an external force to the system, steered molecular dynamics (SMD) simulations coupled with the use of Jarzynski's identity [14,15], can be used to probe the dynamics of biological systems on a timescales more relevant to function and determine the energetics along proposed reaction coordinates [10,16–20]. Insights into the dynamics of these protein systems can further our understanding of the reaction mechanism as well as possible allosteric effects.

HisH–hisF is a multidomain enzyme regulating the fifth step of histidine biosynthesis and is an exquisite example of the complexity of enzymatic catalysis. It also provides a link between two fundamental and diverse metabolic pathways, amino acid metabolism and purine

* Corresponding author. Tel.: +1-217-333-3518; fax: +1-217-244-3186.
E-mail address: schulten@scs.uiuc.edu (Z. Luthey-Schulten).

0301-0104/$ - see front matter © 2004 Elsevier B.V. All rights reserved.
doi:10.1016/j.chemphys.2004.05.019

biosynthesis, through the formation of its two products. HisH, a class-I glutamine amidotransferase, binds one molecule of glutamine in its catalytic triad active-site and hydrolyzes it to form glutamate and ammonia [21]. The nascent ammonia then diffuses roughly 10 Å across the interface of the two docked proteins to a set of four strictly conserved gate residues at the mouth of the hisF barrel. In all species, these four residues form a charge gate comprised of an arginine, a lysine, and two glutamates. In all the available crystal structures, the gate appears to be in a "closed" conformation where the charged residues form salt bridges to one another. Structural and mutational kinetic studies strongly suggest that the gate opens and ammonia passes through the interior of the α–β barrel another 12 Å until it reaches the ribonucleotide hisF substrate *N*′-[(5′-phosphoribulosyl)-formino]-5′ aminoimidazole–carboxamide ribonucleotide (PRFAR) (see Fig. 1). HisF, a cyclase, incorporates the ammonia nitrogen into PRFAR and then cleaves it, resulting in two different products: imidazole glycerol phosphate (a precursor to histidine) and AICAR (the first substrate in the de novo synthesis of purines).

Interestingly, hisH catalytic activity is greatly stimulated (4900-fold) by the binding of PRFAR [22,23]. In fact, crystal structures show that the active-site of hisH has unique structural characteristics that presumably act as a point of control for the amidotransferase reaction. In all available crystal structures, the active-site cysteine is in a energetically unfavorable position, and the characteristic oxyanion hole of hisH is blocked by the backbone carbonyl group of a conserved glycine [11–13]. It is presumed that upon PRFAR binding at the C-terminal end of hisF, a signal is propagated up through hisF and across the interface, thus inducing a reorganization of the hisH active-site that includes both the reorientation of the cysteine as well as the formation of a stable oxyanion hole. The coupled motion may also play a role in coordinating an activated event that leads to motion in the gate residues, thus inducing their opening and allowing ammonia to pass. To date, this reorganization remains uncharacterized and the pathway of communication between the two enzymes has not yet been elucidated. Our bioinformatic analysis representing all three domains of life has revealed a chain of highly conserved residues which lead from the active-site of hisF, along one side of the $(\beta/\alpha)_8$ barrel, up through the interface of the two proteins, and into the active-site of hisH (Fig. 2). It is possible that these residues serve as a communication pathway connecting the two remote active-sites. The final hisF multiple sequence alignment is available at [24].

Since the publication of the yeast structure with substrates, we have parameterized both the covalently bound glutamyl thioester intermediate in hisH as well as the ribonucleotide substrate PRFAR for MD simulations. The current work attempts to model the active-complex for a parallel organism: *Thermatoga maritima*. We have simulated the bacterial enzyme with bound substrates and probed the energetics of the ammonia transport through the hisF barrel, assuming a partially open gate conformation. Our bioinformatics analysis again revealed two highly conserved aspartate residues near the channel gate: Asp-98 near Lys-99 and Asp-219 near Arg-5. If both gate residues Lys-99 and Arg-5 are in alternate rotamer positions, they can form stable ionic contacts with these residues while simultaneously opening the gate to a diameter of 7.0 Å. As the exact

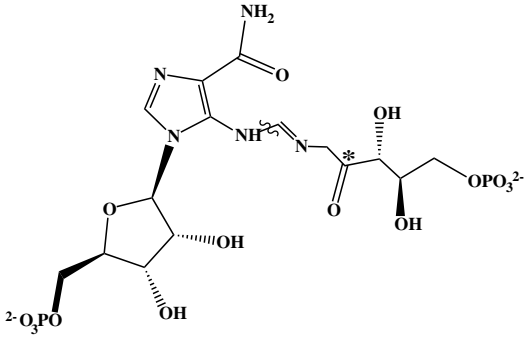

Fig. 1. The labile biphosphate substrate, PRFAR, binds to the C-terminal end of hisF. The asterisk (*) marks proposed site of ammonia attack, and the squiggly line marks the proposed bond cleavage site [8]. The cyclase reaction incorporates the ammonia nitrogen into imidazole glycerol phosphate, a precursor to histidine. The other product of this reaction, AICAR, initiates the de novo synthesis of purines.

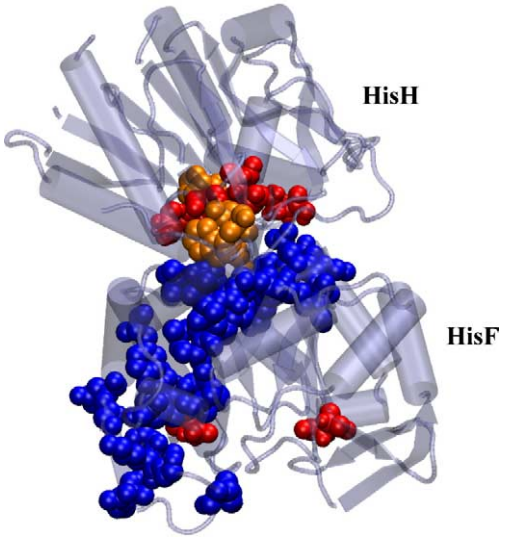

Fig. 2. Highly conserved residues in IGPS (shown in space-filling) form a chain of residues connecting remote active-sites. Active-sites in each protein are shown in red, conserved hisH residues at the interface are shown in orange, conserved hisF residues are shown in blue. The assignment is based on a multiple sequence alignment [24] of 60 SWISS-PROT [54] sequences representing all three domains of life. The covalently bound hisH substrate and the PRFAR substrate of hisF, which were included in the simulations, have been omitted for clarity.

sequence of events is still not understood, we have carried out similar simulations on both the partially open and the proposed fully open-gate conformations. The active-complex simulations also provide new insights into the effects of water molecules at the interface near the gate opening; specifically, we have investigated their effects on the energetics of ammonia transport through the gate region.

2. Methods

2.1. Modeling the active-complex

The crystal structure used in the simulations is the *T. maritima* structure (Protein Data Bank code 1GPW) without substrates. System setup was similar to that described in an earlier study [10], except that the current system was modified to resemble an activated complex. Chains C and D of the hisH–hisF complex were chosen because the loop on the C-terminal end of hisF was resolved in a closed (assumed active) conformation. Loop "switching" on the C-terminal end of α–β barrels is a common functional control motif. To date, the best characterized system is loop six of triosephosphate isomerase, which has been shown to close around its biphosphate substrate and then reopen for product release; this loop switching motion has been reported to occur on the millisecond timescale [25–27]. It is evident from the available crystal structures that the loop after the first β strand in hisF undergoes a structural transition from a disordered *apo*-state to an ordered *active*-state when PRFAR binds. This structural transition involves the formation of two anti-parallel β strands that make contact with the bound PRFAR substrate. The formation of secondary structure elements from a disordered state is a signaling mechanism used in response to cellular hypoxia [28], and structural evidence of IGPS strongly suggests a similar type of mechanism may be involved in its signaling event. This structured, closed loop is present in the archaeal [29] and bacterial structures, however PRFAR was not resolved. In the yeast structure with the resolved PRFAR, some residues of the switching loop are missing. In the bacterial crystal structures where the switching loop of hisF was seen in a closed, ordered conformation, two phosphates were also crystallized in the phosphate binding sites at the C-terminal end of the barrel. In chain E of the same PDB file, the loop is in a disordered, more open conformation and there are no phosphates present. As PRFAR was present in the crystal solution, one can assume the phosphates bound to the bacterial structures were from an unresolved PRFAR molecule, further suggesting a structured loop transition upon substrate binding.

Building both substrates into the system introduced two non-standard residues into the simulations. We modeled the hisH substrate as a covalently bound glutamyl thioester intermediate to Cys-84 of the active site; according to the mechanism, this is consistent with a post-ammonia release state [30,31]. Parameterization was performed on the thioester linkage [32]. Including the bound PRFAR in the simulations presented a more challenging parameterization project (see Fig. 1). The parameterization of the ribonucleotide substrate was performed following the established CHARMM protocol [33–35]. The substrate was broken into smaller fragments already available in the CHARMM27 topology and parameter files, and the parameters for the linkages determined from quantum chemistry calculations. Placement of PRFAR into the bacterial structure was done by aligning the original phosphate molecules present in the bacterial crystal structure with the phosphates from the crystallized PRFAR. The end-to-end distance of the crystallized PRFAR from yeast aligned nearly perfectly with the previously crystallized phosphates in *T. maritima*, again suggesting that indeed PRFAR may have been bound to hisF, but been too unstable to resolve.

It is clear from biochemical studies on the complex that the two reactions at the hisH and hisF active-sites are tightly coupled. The activity of hisH is greatly stimulated by the presence of the hisF substrate PRFAR [22,23], yet little is known about the exact mechanism regarding the allosteric interactions. One obvious implication of the available crystal structures and the energetic analysis of the apo-complex is that there seems to be a gating mechanism whereby the strictly conserved gate residues must undergo some kind of structural transition that allows the gate to open and ammonia to pass [10]. Aside from mutational studies, to date there has not yet been any experimental characterization of the gating mechanism. In our initial studies of the apo-complex and in the first set of simulations for the active-complex, we followed a suggestion put forth in [12] where Lys-99 of the gate was held fixed in an open position allowing it to hydrogen bond with conserved Tyr-138 of hisH [10]. Additionally, in one of the bacterial crystal structures, Lys-99 was reported in slightly different conformations, which suggests that it may be involved in the gate opening motion [11]. We refer to this particular gate conformation as the *partially open* gate.

In order to model a more open-gate conformation, both Lys-99 and Arg-5 were put into alternate low-lying rotamer conformations that allow them to form stable salt bridges with nearby conserved Asp-98 and Asp-219 of hisF (referred to as the *fully open*-gate). The rotamer states were motivated by energetic and bioinformatic considerations [10], and a complete multiple sequence alignment of IGPS from all three domains of life is available as supplementary information [24]. The χ_1 to χ_4 rotamer angles of the fully open-gate for Arg-5 are -62, -165, -57, -66 and of Lys-99 are -36, -62, -164, -54.

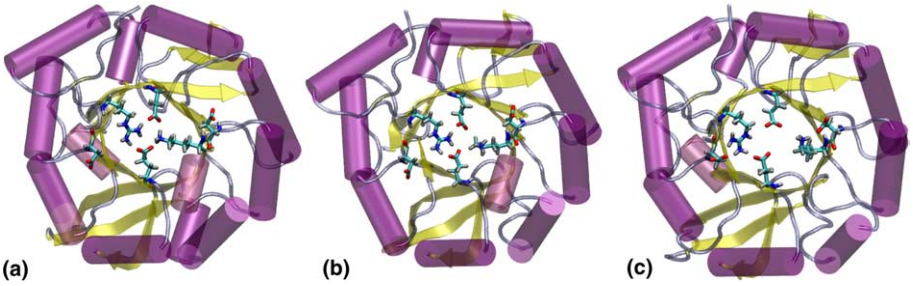

Fig. 3. A top view of the N-terminal side of hisF shows the gate residues Arg-5, Glu-46, Lys-99, and Glu-167 in different conformations. (a) Closed gate configuration present in crystal structures (hydrogens added) allows a 3.2 Å diameter opening for ammonia transport. (b) Partially open-gate simulated in [10] and again with substrates with a 5.8 Å diameter opening; Lys-99 is rotated to hydrogen bond with conserved Tyr-138 in hisH. (c) Proposed fully open gate configuration with a 7.0 Å diameter opening; Arg-5 rotated to form a salt bridge with Asp-219, Lys-99 rotated to form a salt bridge with Asp-98.

The diameter of this fully open-gate was 7 Å after minimization (a comparison of all gate conformations is presented in Fig. 3). During the minimization, both residues remained in their open-gate rotamers; during equilibration, however, Arg-5 shifted back to the closed conformation after 200 ps. It is obvious from the available biochemical studies that Arg-5 plays an essential role in the gating mechanism; any mutation made to the residue destroys the cyclase reaction while the amidotransferase reaction is unaffected [23]. Though Lys-99 is also strictly conserved, mutations of Lys-99 to an arginine do not seem to affect the cyclase reaction or overall reaction kinetics, though it has been reported that mutating Lys-99 to an alanine results in loss of ammonia, presumably because of improper gating function [8]. It is for this reason and also because we wanted to simulate a more open-gate conformation that we held Arg-5 fixed in the open rotamer position. Since Lys-99 remained in the stable salt bridge to Asp-98, no conformational constraints were applied to it.

2.2. Simulation parameters

Active-site residues in both subunits were analyzed according to available biochemical information. For hisH, His-178 of the catalytic triad is unprotonated in order to be consistent with a covalently bound glutamine to Cys-84 in the active-site [30,31]. For hisF, the original crystal structure has an active-site mutation that we mutated back to its wild-type form (D11N). All crystal waters were kept and DOWSER [36] was used to augment the crystal water molecules in the interface; water molecules contributing favorably above a potential energy cutoff were included in the simulation. Hydrogens were added with PSFGEN and explicit solvent was added with SOLVATE [37] through VMD [38].

The composite 48,816 atom system was equilibrated for 1 ns in the NPT ensemble, using periodic boundary conditions and the Langevin piston method [39] to control pressure at 1 atm. Particle Mesh Ewald was used to efficiently treat electrostatics without a cutoff [40]. Temperature was held constant at 298 K and the time step was 1 fs. All of the simulations including the SMD trajectories were performed with NAMD2 [41] using the CHARMM27 forcefield [33] and the TIP3 water model [42]. Simulations were performed on Pittsburgh Supercomputing Center's LeMieux platform with 128-processors and on our local 46-processor Linux-i686-Scyld cluster. Each ammonia pulling trajectory was performed in the NVT-ensemble and each 1.25-ns simulation took ≈12 h on LeMieux or 24 h on the local machine.

We pulled ammonia through the channel with constant-velocity SMD, but for this study we reduced the pulling speed from 15 Å/ns, used in the study of the apo-complex, to 10 Å/ns. This reduction in pulling velocity is consistent with a recent recommendation that fewer, slow trajectories give more accurate estimates for free energy profiles reconstructed with Jarzynski's identity better than more, fast ones [20]. The time-dependent external force is added to the system's original Hamiltonian: $H[\underline{x}(t),t] = H_0[\underline{x}(t)] + 0.5k[z(\underline{x}) - z_0 - vt]^2$, where v is the velocity of the harmonic constraint used to pull the ammonia, z_0 is the initial position of the center of mass of ammonia, and $z(\underline{x})$ is the position of the center of mass of ammonia at time t. For all simulations, we chose a harmonic constraint of $k = 150$ pN/Å, which is stiff enough to constrain the ammonia along the channel reaction path while simultaneously allowing it to interact with its environment. Jarzynski's identity, $e^{-\beta\Delta F} = \langle e^{-\beta\Delta \mathscr{W}} \rangle_{\text{traj}}$ can be used to extract equilibrium free energy information from these repeated non-equilibrium pulling simulations, where the averaged work is actually the total work minus the instantaneous biasing potential $\mathscr{W}(t) = W(t) - 0.5k[z(\underline{x}(t)) - vt]^2$. The free energy profile along the channel reaction coordinate was ultimately reconstructed following the methods in [17] which pioneered the use of the second-order cumulant expansion to approximate the exponential average [10].

The use of the second-order cumulant in the reconstruction of free energy profiles and Jarzynski's identity has been the subject of several recent papers [18–20].

3. Results and discussion

3.1. Effect of substrates on ammonia conduction

Characterizing the energetics of biological systems is central to understanding how these systems work. An increasingly popular tool for energetic analysis in numerical statistical mechanics is the application of Jarzynski's identity, which permits one to extract unperturbed free energy profiles from repeated non-equilibrium force measurements [14,15]. Recently, SMD simulations and single-molecule RNA microscopy experiments have been successfully used to reconstruct free energy profiles through the use of this new technique [10,17,18,43]. In our previous simulations of hisH–hisF, we showed how the free energy profile was obtained from the force measurements. In this report, we use the Jarzynski identity to infer the energetics of the activated complex from the force curves without explicitly reconstructing the free energy profiles. For comparison purposes we simulated the partially open-gate conformation previously considered [10], as well as a newly proposed fully open-gate conformation. The only difference between the sets of partially open-gate simulations is the presence of substrates in the active-complex.

The bound substrates have a pronounced effect on ammonia conduction as evidenced from the resulting force curves and electrostatic maps of the activated complex. In the partially open-gate trajectories, the barrier for ammonia to pass through the gate is considerably higher when the substrates are present (see Fig. 4). In all of these trajectories, ammonia passes through the gate very close to the geometric center of the opening, close to Lys-99, and it is almost always in the same position when it passes with the nitrogen facing towards Lys-99. The orientation of ammonia at the gate is identical in both sets of simulations. The larger barrier to ammonia entry was surprising until the local electrostatic environment was examined. DelPhi electrostatic calculations revealed that the presence of substrates dramatically changes the electrostatic environment within the channel and interface [44]. When the substrates are bound, the entire α–β barrel and interface become more negatively charged; this effect is illustrated in Fig. 5. This result is hardly surprising as the biphosphate PRFAR carries an overall charge of −4e, and the covalently bound glutamyl thioester intermediate, which protrudes into the interface of the two proteins, carries a charge of −1e. A dipole analysis of ammonia at the interface, before ammonia passes through the gate, reveals

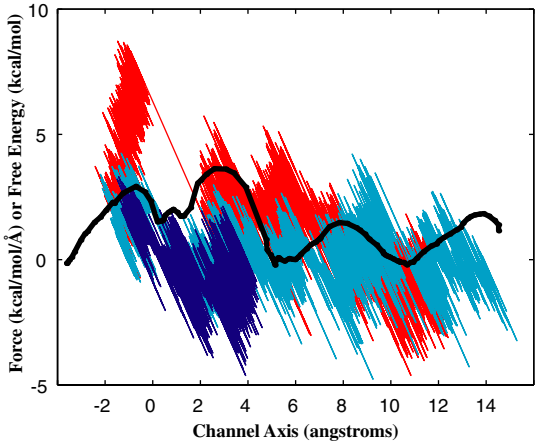

Fig. 4. Force and free energy profiles as a function of the ammonia position along the barrel axis. The smooth black line is the free energy profile of the partially open apo-complex [10] and the cyan line is a representative force curve used to generate the energy profile; the first minimum (near 1 Å on the channel axis) corresponds to the position of Thr-78, the second minimum (near 6 Å on the channel axis) corresponds to the position of Ser-101. For reference, in the active-complex simulations, PRFAR is located at 12 Å on the channel axis. The red line is a representative force curve from the partially open-gate conformation of the active-complex, and the dark blue line is a representative force curve from the fully open-gate conformation of the active-complex. In all trajectories, there was only one water molecule inside the first vestibule of the channel.

that the preferred orientation of ammonia in both the apo- and active-complexes is with the hydrogens facing towards the gate residues. When ammonia passes through the gate, however, it rotates so that the nitrogen faces towards Lys-99. When the substrates are present, the local electrostatic field opposes the reorientation of the dipole moment, making it energetically unfavorable to enter the channel.

The 8–10 kcal/mol/Å force requirement for ammonia entry in the partially open active-complex suggested that an alternate, more open gate conformation should be considered. A multiple sequence alignment of IGPS sequences from all three domains of life revealed that there are two conserved aspartate residues near the channel gate. A study of possible energetically low-lying rotamer states of the four gate residues suggested that Arg-5 and Lys-99 could be in alternate rotamer states that would allow them to simultaneously form salt bridges with the two conserved aspartates while opening the diameter of the gate to 7.0 Å [10]. This proposed fully open-gate conformation did indeed require significantly lower forces to ammonia entry, ≈2.5 kcal/mol/Å. While the fully open-gate mechanism is hypothetical, it strongly suggests more than one of the gate residues and possibly additional nearby conserved residues are involved in the gate opening mechanism.

The behavior of water in the gate region and in the channel is different, and water has distinct contributions

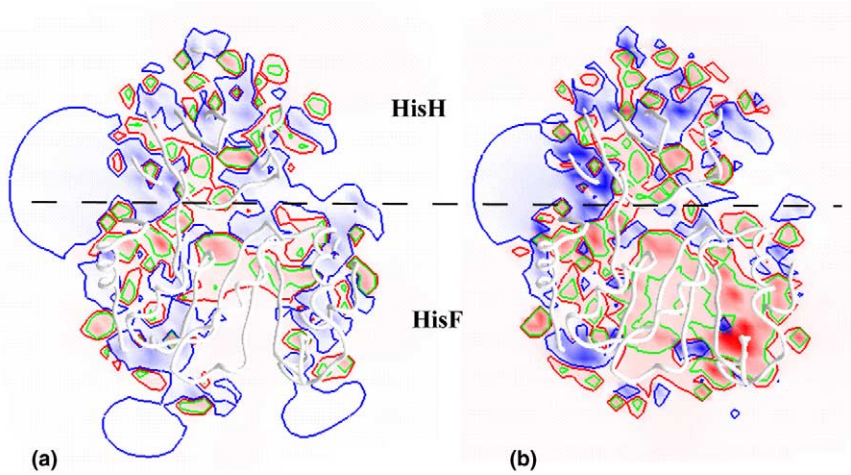

Fig. 5. DelPhi electrostatic potential map of IGPS generated from DelPhi v. 4 [44]. The charges are assigned from CHARMM27 using a dielectric constant of 2.0 in the interior of the protein and 78 outside. The dashed black line denotes the interface between the hisH and hisF domains. Blue shading corresponds to positive potential, red shading corresponds to negative potential. Isopotential lines for both pictures are defined at: 0 (blue), −10 (red), −20 (green). Slice along the barrel axis of (a) the apo-complex and (b) the active-complex.

to the force curves depending on the location of ammonia along the reaction coordinate. *Within the channel*, the behavior of water in the active-complex differs from that in the apo-complex. The trajectories of the active-complex show that there is a direct competition for hydrogen bonding with ammonia between the few conserved polar groups lining the channel and any nearby water molecules. In particular, while ammonia is interacting with the conserved Thr-78, it must wait for one or two bulk water molecules to make their way around PRFAR and diffuse up to ammonia before the ammonia can travel any further down the channel. At this point, the ammonia molecule breaks its hydrogen bond with Thr-78, makes a new hydrogen bond with the water molecule, and continues its transport through the channel. The breaking of the hydrogen bond with Thr-78 corresponds to the second maximum in the force curves. The third maximum represents the breaking of the hydrogen bond between ammonia and conserved Ser-101. Ser-101 is located two-thirds of the way down the barrel and once ammonia passes this residue, it is within 3 Å of PRFAR. In the apo-complex trajectories, ammonia also formed hydrogen bonds to the water molecule(s) in the channel [10], but without PRFAR bound across the C-terminal end of the barrel, bulk water molecules were able to diffuse in more freely. The presence of PRFAR, which physically blocks the bulk water molecules from freely diffusing up into the channel, actually increases the barriers within the channel by making ammonia wait for alternate hydrogen bonding partners. It is also interesting to note that once ammonia has broken its hydrogen bond with Ser-101 and is close to PRFAR, negative forces have to be applied in order to slow it down. Compared to simulations of the apo-complex, the forces in this region are considerably lower and reveal the attractive interactions between ammonia and PRFAR.

3.2. Effect of water molecules in the gate region

The significance of the roles that water molecules play in biological function cannot be overstated: they assist in enzyme catalysis, lubricate protein–protein interfaces [45], and even control the passage of protons through membrane proteins [46,47]. Full-atom MD simulations allow us to monitor the behavior of water molecules at specific points in the protein system. It has been argued that in order to keep the ammonia from becoming protonated (thereby losing its nucleophilic character which is required for the subsequent cyclase reaction) the interface and channel of IGPS need to be hydrophobic environments [23,11], or at least provide a pathway for ammonia transport that is free from exchange with bulk solvent [8]. As hydrophobic substrate channels have been found in other glutamine amidotransferases, it seems that shielding the ammonia from bulk solvent is a common mechanism among the amidotransferases [30,48–53]. A close examination of the IGPS crystal structures reveals that although the interface between hisH and hisF is predominantly hydrophobic, it has 12–18 water molecules in the interface depending on the specific PDB entry. A comparison of five PDB images of the complex from yeast and bacterial structures revealed that, not surprisingly, there are even variations in the number of water molecules present within the hydrophobic channel. In three of the structures, there is one water molecule just inside the channel near the four gate residues. In one of the images, there are no water molecules present, and in another there are two. For all of the partially open-gate simulations, we

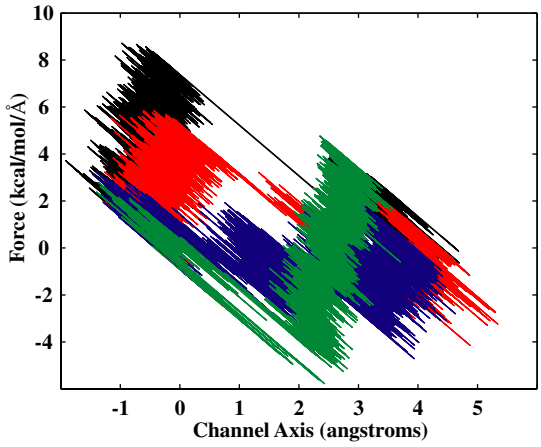

Fig. 6. Force curves for pulling ammonia through the channel gate entrance for various hydration states. Black corresponds to three water molecules inside the first vestibule of the channel, red corresponds to two, blue to one, and green has no water molecules.

chose to simulate the complex with one water molecule inside the channel since the majority of crystal structures had that configuration. Interestingly, during the equilibration of the fully open-gate conformation, two additional water molecules spontaneously entered the channel (for proper positioning, the ammonia nitrogen was held fixed during the equilibration and so did not enter the channel).

During the pulling simulations, we initially kept all three water molecules that were present inside the first vestibule of the channel at the end of the equilibration run. The result was a much higher barrier to ammonia entry through the fully open-gate conformation, as high as 10 kcal/mol/Å, shown in Fig. 6. As none of the crystal structures have three water molecules inside the channel, and there has not yet been a systematic study of the water at the interface, we decided to simulate alternate hydration states in order to probe the effect of the number of water molecules on the barrier to ammonia entry. The results are illustrated in Fig. 6. From the force curves, it is clear that as the number of water molecules decreases, so do the forces required for ammonia entry.

The trajectories show that when there are three water molecules inside the channel, they physically block ammonia from entering. In order to pull ammonia into the channel, the water molecules have to be displaced; they either exit the channel or move further down into the barrel. However, to move further into the hydrophobic barrel, the water molecules must break their hydrogen bond network; the corresponding energetic penalty is reflected in the resultingly higher force curves. With two water molecules, the result is similar but not as dramatic. When there is only one water molecule inside the channel, ammonia can easily make its way through the fully open-gate conformation without having to displace any water molecules. The presence of one water molecule makes it easier for ammonia to translate further down into the channel because the water molecule provides ammonia with an alternate hydrogen bonding partner. As mentioned previously, there is always a competition for hydrogen bonding between ammonia and the protein or a nearby water molecule(s). As ammonia moves through the channel from one polar residue to the next, it utilizes the nearby water molecule as a bridge to assist it in making large translational moves without sacrificing a hydrogen bond. When the channel has no water molecules, it is very easy for ammonia to pass through the fully open-gate; Fig. 6 shows negative forces being applied to ammonia in this case. Since the simulations were run in the constant-velocity regime, the application of negative forces means forces were applied to slow the ammonia down, or in other words, ammonia was actually being pulled down through the gate faster than 10 Å/ns. However, without a water molecule to provide an alternate hydrogen bonding partner, much larger forces are required to pull the ammonia any further into the barrel. Therefore, we predict that the most favorable water configuration is when there is one water molecule just inside the channel gate, which is the most probable state seen in the crystal structures.

The fact that two water molecules spontaneously entered the channel when the gate was fixed in the fully open position, coupled with the energetic analysis, leads to two interesting implications. First it suggests that the gate most likely does not remain in the open position for long periods of time (i.e. it is probably a short-lived event). Second, it implies that indeed the interface needs to be at least somewhat hydrophobic to prevent any additional water molecules from entering the channel before ammonia does. The latter implication strongly supports the notion that in addition to the loop switching motion upon PRFAR binding, the interface of the two proteins may need to "tighten" in order to expel excess bulk water molecules and provide a more sequestered environment for ammonia transport [13,8]. Although the presence of substrates does increase fluctuations in the motion of the gate residues (data not shown), there is no significant "gate-opening" motion seen, even with several nanoseconds of unconstrained equilibration. Our simulations suggest that more likely the gate opening is part of a short-lived activated event coupled to the allosteric signal initiated by PRFAR binding at the hisF active-site.

4. Conclusions

We have used steered molecular dynamics simulations to probe the energetics of ammonia channeling in the metabolic enzyme, IGPS, for both apo- and active-complexes. Binding of the hisF substrate PRFAR alters

the internal electrostatic field and dramatically changes the energetics of ammonia conduction at the channel gate, as well as along the interior of the barrel. Motivated by a bioinformatic analysis, we simulated a newly proposed open-gate configuration, and predicted from both topological and energetic considerations, several additional residues are involved in the gating mechanism. These simulations also present the first systematic study of the effects of water molecules both at the interface and within the hisF channel. Our results clearly argue for a more hydrophobic environment at the interface and within the channel and suggest that the optimum number of water molecules inside the barrel is one. The presence of only one water molecule provides ammonia with a necessary alternate hydrogen bonding partner without blocking its entrance into the barrel.

Acknowledgements

We thank the Theoretical and Computational Biophysics Group at the Beckman Institute, University of Illinois, for kindly allowing us to use their computational resources, as well as for many insightful discussions. This work was funded by National Science Foundation Grant MCB02-35144 and a National Resource Allocation Grant MCA0350275.

References

[1] N. Nagano, C. Orengo, J.M. Thornton, J. Mol. Biol. 321 (2002) 741.
[2] J.A. Silverman, R. Balakrishnan, P.B. Harvey, Proc. Natl. Acad. Sci. USA 98 (2001) 3092.
[3] Y. Wu, C.R. Matthews, J. Mol. Biol. 330 (2003) 1131.
[4] D. Lang, R. Thoma, M. Henn-Sax, R. Sterner, M. Wilmanns, Science 289 (2001) 1546.
[5] C. Jurgens, A. Strom, D. Wegener, S. Hettwer, M. Wilmanns, R. Sterner, Proc. Natl. Acad. Sci. USA 97 (2000) 9925.
[6] J.A. Gerlt, P.C. Babbitt, Ann. Rev. Biochem. 70 (2001) 209.
[7] G. Jogl, S. Rozovsky, A.E. McDermott, L. Trong, Proc. Natl. Acad. Sci. USA 100 (2003) 50.
[8] R. Myers, J. Jensen, I. Deras, J. Smith, V.J. Davisson, Biochemistry 42 (2003) 7013.
[9] R.K. Wierenga, FEBS Lett. 492 (2001) 193.
[10] R. Amaro, E. Tajkhorshid, Z. Luthey-Schulten, PNAS 100 (2003) 7599.
[11] A. Douangamath, M. Walker, S. Beismann-Driemeyer, M. Vega-Fernandez, R. Sterner, M. Wilmanns, Structure 10 (2002) 185.
[12] B. Chaudhuri, S. Lange, R. Myers, S. Chittur, V.J. Davisson, J.L. Smith, Structure 9 (2001) 987.
[13] B.N. Chaudhuri, S.C. Lange, R.S. Myers, V.J. Davisson, J.L. Smith, Biochemistry 42 (2003) 7003.
[14] C. Jarzynski, Phys. Rev. E 56 (1997) 5018.
[15] C. Jarzynski, Phys. Rev. Lett. 78 (1997) 2690.
[16] G. Hummer, A. Szabo, Proc. Natl. Acad. Sci. USA 98 (2001) 3658.
[17] M.O. Jensen, S. Park, E. Tajkhorshid, K. Schulten, Proc. Natl. Acad. Sci. USA 99 (2002) 11175.
[18] S. Park, F. Khalili-Araghi, E. Tajkhorshid, K. Schulten, J. Chem. Phys. 119 (6) (2003) 3559.
[19] J. Gore, F. Ritort, C. Bustamante, Proc. Natl. Acad. Sci. USA 100 (2003) 12564.
[20] S. Park, K. Schulten, J. Chem. Phys. 120 (2004) 5946.
[21] J.J. Tesmer, T.J. Klem, M.L. Deras, V.J. Davisson, J.L. Smith, Nat. Struct. Biol. 3 (1996) 74.
[22] T. Klem, V. Davisson, Biochemistry 32 (1993) 5177.
[23] S. Beismann-Driemeyer, R. Sterner, J. Biol. Chem. 276 (2001) 20387.
[24] R. Amaro, A. Sethi, Zan Luthey-Schulten, Supplemental Information Website HisF Multiple Sequence Alignment. Available from <http://www.scs.uiuc.edu/schulten/>, 2004.
[25] S. Rozovsky, G. Jogl, L. Tong, A.E. McDermott, J. Mol. Biol. 310 (2001) 271.
[26] S. Rozovsky, A.E. McDermott, J. Mol. Biol. 310 (2001) 259.
[27] R. Desamero, S. Rozovsky, N. Zhadin, A. McDermott, R. Callender, Biochemistry 42 (2003) 2941.
[28] S.A. Dames, M. Martinez-Yamout, R.N.D. Guzman, H.J. Dyson, P. Wright, Proc. Natl. Acad. Sci. USA 99 (2002) 5271.
[29] M. Banfield, J.S. Lott, V. Arcus, A. McCarthy, E. Baker, Acta Cryst. D 57 (2001) 1518.
[30] F.M. Raushel, J.B. Thoden, H.M. Holden, Biochemistry 38 (1999) 7891.
[31] J.B. Thoden, X. Huang, F.M. Raushel, H.M. Holden, Biochemistry 38 (1999) 16158.
[32] R. Amaro, F. Autenrieth, J. Baudry, R. Braun, Z. Luthey-Schulten, Determining forcefields, available from <http://www.ks.uiuc.edu/Training/SumSchool/materials/sources/tutorials/06-forcefield/forcefield-html>, 2003.
[33] A.D. MacKerell, D. Bashford, M. Bellott, R.L. Dunbrack, J.D. Evanseck, M.J. Field, S. Fischer, J. Gao, H. Guo, S. Ha, D. Joseph-McCarthy, L. Kuchnir, K. Kuczera, F.T.K.L.C. Mattos, S. Michnick, T. Ngo, D.T. Nguyen, B. Prodhom, W.E. III, B. Roux, M. Schlenkrich, J.C. Smith, R. Stote, J. Straub, M. Watanabe, J. Wiorkiewicz-Kuczera, D. Yin, M. Karplus, All-atom empirical potential for molecular modeling and dynamics studies of proteins, J. Phys. Chem. B 102 (1998) 3586.
[34] A. MacKerell, Workshop on methods and applications of molecular dynamics to biopolymers. Available from <http://www.psc.edu/general/software/packages/charmm/tutorial/index.html>, 2003.
[35] A. MacKerell, Parameterization of molecules for use of CHARMM. Available from <http://www.psc.edu/general/software/packages/charmm/tutorial/mackerell/parameters.html>, 2003.
[36] L. Zhang, J. Hermans, PROTEINS: Struct. Func. Genetics 24 (1996) 433.
[37] H. Grubmuller, Solvate, Theoretical Biophysics Group Institute for Medical Optics, Ludwig-Maximilians University, Munich, Version 1.0.
[38] W. Humphrey, A. Dalke, K. Schulten, J. Mol. Graph. 14 (1996) 33.
[39] S. Feller, Z. Zhang, R. Pastor, B. Brooks, J. Chem. Phys. 103 (1995) 4613.
[40] T. Darden, D. York, L. Pedersen, J. Chem. Phys. 98 (1993) 10089.
[41] L. Kale, R. Skeel, M. Bhandarkar, R. Brunner, A. Gursoy, N. Krawetz, J. Phillips, A. Shinozaki, J. Comp. Phys. 151 (1999) 283.
[42] W.L. Jorgensen, J. Chandrasekhar, J.D. Madura, R.W. Impey, M.L. Klein, J. Chem. Phys. 79 (1983) 926.
[43] J. Liphardt, S. Dumont, S.B. Smith, I.T. Carlos Bustamante Jr., Science 296 (2002) 1832.
[44] W. Rocchia, E. Alexov, B. Honig, J. Phys. Chem. B 105 (2001) 6507.
[45] G. Papoian, J. Ulander, P. Wolynes, J. Am. Chem. Soc. 125 (2003) 9170.
[46] R. Pomes, B. Roux, Biophys. J. 75 (1998) 33.
[47] E. Tajkhorshid, P. Nollert, M. Jensen, L.J. Miercke, J. O'Connell, R.M. Stroud, K. Schulten, Science 296 (2002) 525.

[48] J.M. Krahn, J.H. Kim, M.R. Burns, R.J. Parry, H. Zalkin, J.L. Smith, Biochemistry 36 (1997) 11061.
[49] A. Teplyakov, G. Obmolova, B. Badet, M.-A. Badet-Denisot, J. Mol. Biol. 313 (2001) 1093.
[50] J.B. Thoden, H.M. Holden, G. Wesenberg, F.M. Raushel, I. Rayment, Biochemistry 36 (1997) 6305.
[51] C. Binda, R.T. Bossi, S. Wakatsuki, S. Artz, A. Coda, B. Curti, M.A. Vanoni, A. Mattevi, Structure 8 (2000) 1299.
[52] T.M. Larsen, S.K. Boehlein, S.M. Schuster, N.G.J. Richards, J.B. Thoden, H.M. Holden, I. Rayment, Biochemistry 38 (1999) 16146.
[53] J. Kim, F.M. Raushel, Biochemistry 43 (2004) 5334.
[54] R. Apweiler, A. Bairoch, C. Wu, W. Barker, B. Boeckmann, S. Ferro, E. Gasteiger, H. Huang, R. Lopez, M. Magrane, M. Martin, D. Natale, C. O'Donovan, N. Redaschi, L. Yeh, Nucleic Acids Res. 32 (2004) D115.